Single sensor boost converter-based maximum power point tracking algorithms

Caston Urayai, and Gehan A. J. Amaratunga
Electrical Engineering Division, Engineering Dept.
Cambridge University
Cambridge, UK
cu211@cam.ac.uk, gaja1@cam.ac.uk

***Abstract*—Two new maximum power point tracking algorithms are presented: the input voltage sensor, and duty ratio maximum power point tracking algorithm (ViSD algorithm); and the output voltage sensor, and duty ratio maximum power point tracking algorithm (VoSD algorithm). The ViSD and VoSD algorithms have the features, characteristics and advantages of the incremental conductance algorithm (INC); but, unlike the incremental conductance algorithm which requires two sensors (the voltage sensor and current sensor), the two algorithms are more desirable because they require only one sensor: the voltage sensor. Moreover, the VoSD technique is less complex; hence, it requires less computational processing. Both the ViSD and the VoSD techniques operate by maximising power at the converter output, instead of the input. The ViSD algorithm uses a voltage sensor placed at the input of a boost converter, while the VoSD algorithm uses a voltage sensor placed at the output of a boost converter.**

I. INTRODUCTION

Maximum power point tracking (MPPT) has become an indispensible part of photovoltaic (PV) systems. This is because, it operates solar panels at the maximum power point (MPP) — the point at which a solar panel delivers the most power at any point in time — thereby maximising PV energy extraction, and in turn increasing PV system efficiency. Resultantly, various MPPT techniques with different characteristics and performances have been proposed in the past [1].

In [2] and [3], the almost linear relationship under varying atmospheric conditions, between V_{oc} (solar panel open-circuit voltage) and V_{MPP} (solar panel voltage at MPP), or between I_{sc} (solar panel short-circuit current) and I_{MPP} (solar panel current at MPP), is used. By periodically measuring V_{oc} or I_{sc}, and applying this linear relationship relationship, V_{MPP} or I_{MPP} is determined respectively. Although this method is simple and cheap, it is prone to inaccuracy as PV modules age. The method is an approximation; hence does not operate the solar panel at the maximum power point. Moreover, there is temporary loss of power due to the momentary shut down of the system during the measurement of V_{oc} or I_{sc}.

In the perturb and observe (PO) method [4] – [6], PV module voltage or current is increased/decreased and its output power measured. If the new power measurement is higher, module voltage or current is further increased/decreased otherwise the opposite perturbation is done to the module voltage or current. This method automatically takes into account the effects of PV module aging, because of closed-loop tracking. Because of the nature of tracking, PV module output power oscillates around the maximum power point leading to power losses and reduced efficiency. To measure output power, two sensors are usually required to measure module voltage and current. Some researchers have tried to mitigate some of the PO method drawbacks, but this has resulted in added complexity.

The incremental conductance (INC) method [7] – [10] periodically measures PV module voltage and current, and then tracks the maximum power point by driving the sum of instantaneous conductance and incremental conductance to zero. This method is faster than the PO method, albeit with a modest increase in control system complexity. Two sensors are necessary for periodic measurements of voltage and current.

Fuzzy logic [1] and [11] uses three stages: fuzzification, table lookup and defuzzification for maximum power point tracking. During fuzzification, numerical variables are converted into linguistic variables using a membership function. A lookup table is then used to generate output linguistic variables. The defuzzification stage then converts the linguistic variables to numerical variables which are then used in the power converter control system. This technique performs well under varying atmospheric conditions and is highly responsive, but complexity and costs are a major drawback.

In the neural network method [1] and [12], a neural network — composed of three layers: input, hidden and output — is used. Input variables can be parameters such as irradiance. The output can be the converter duty ratio. The neural network is trained for a particular PV module over a long time. Relationship patterns between the input and output variables are then recorded in the neural network, and algorithms stocked in the hidden layer. The speed of tracking the maximum power point is fast. Like the fuzzy logic method, this method suffers from high complexity and costs. Besides that, the open loop nature of maximum power point tracking makes this technique susceptible to module aging effects.

978-1-4244-8085-2/11/$26.00 ©2011 IEEE

By and large, the PO and INC methods or their variations are widely used. Of the two, the INC algorithm is more desirable because its faster and more accurate. Because the ViSD and VoSD techniques' operational characteristics are similar to those of the INC algorithm, they have the same advantages as the INC method over the PO method. Compared to both the PO and INC methods, the ViSD and VoSD techniques eliminate the use of the more costly and complex current sensor by using only the voltage sensor. This results in reduced costs and circuit complexity.

II. THEORY

A. ViSD algorithm

Power p_o delivered by a boost converter to a load R is given by,

$$p_{\mathrm{o}} = \frac{{v_{\mathrm{o}}}^2}{R} \tag{1}$$

where v_o is the voltage at the converter output terminals. From (1), maximum power $p_{o(max)}$ is delivered at maximum output voltage $v_{o(max)}$.

Hence, at the point of maximum power delivery to the load,

$$\frac{\mathrm{d}p_{\mathrm{o}}}{\mathrm{d}t} = \frac{\mathrm{d}v_{\mathrm{o}}}{\mathrm{d}t} = 0. \tag{2}$$

For a boost converter in continuous conduction mode, the relation in (3) holds,

$$v_{\mathrm{o}} = \frac{v_{\mathrm{i}}}{1-D} \tag{3}$$

where v_i is the voltage at the converter input terminals and D is the converter duty ratio.

Applying the relation in (3), to (2),

$$\frac{\mathrm{d}v_{\mathrm{o}}}{\mathrm{d}t} = \frac{\mathrm{d}(\frac{v_{\mathrm{i}}}{1-D})}{\mathrm{d}t} = 0 \tag{4}$$

$$\frac{(1-D)\frac{\mathrm{d}v_{\mathrm{i}}}{\mathrm{d}t} - v_{\mathrm{i}}\frac{\mathrm{d}(1-D)}{\mathrm{d}t}}{(1-D)^2} = 0 \tag{5}$$

$$\frac{\mathrm{d}v_{\mathrm{i}}}{\mathrm{d}D} = -\frac{v_{\mathrm{i}}}{1-D} \tag{6}$$

Therefore, the condition in (6) holds true at the point at which a boost converter in continuous conduction mode delivers maximum power to a load. Designing a boost converter operating in continuous conduction mode is described in [13] and [14].

B. VoSD algorithm

An even simpler algorithm can be obtained by replacing v_i in (6) with v_o. Equation (7) is then obtained,

$$\frac{\mathrm{d}\big(v_{\mathrm{o}}(1-D)\big)}{\mathrm{d}D} = -\frac{v_{\mathrm{o}}(1-D)}{D} \tag{7}$$

$$\frac{\mathrm{d}v_{\mathrm{o}}}{\mathrm{d}D} - \frac{\mathrm{d}(v_{\mathrm{o}}D)}{\mathrm{d}D} = -\frac{v_{\mathrm{o}}(1-D)}{D} \tag{8}$$

On simplifying,

$$\frac{\mathrm{d}v_{\mathrm{o}}}{\mathrm{d}D} = 0 \tag{9}$$

Therefore, the condition in (8) holds true at the point at which a boost converter in continuous conduction mode delivers maximum power to a load.

Fig. 1 and 2 show the ViSD and VoSD algorithms' control flow chart algorithms respectively.

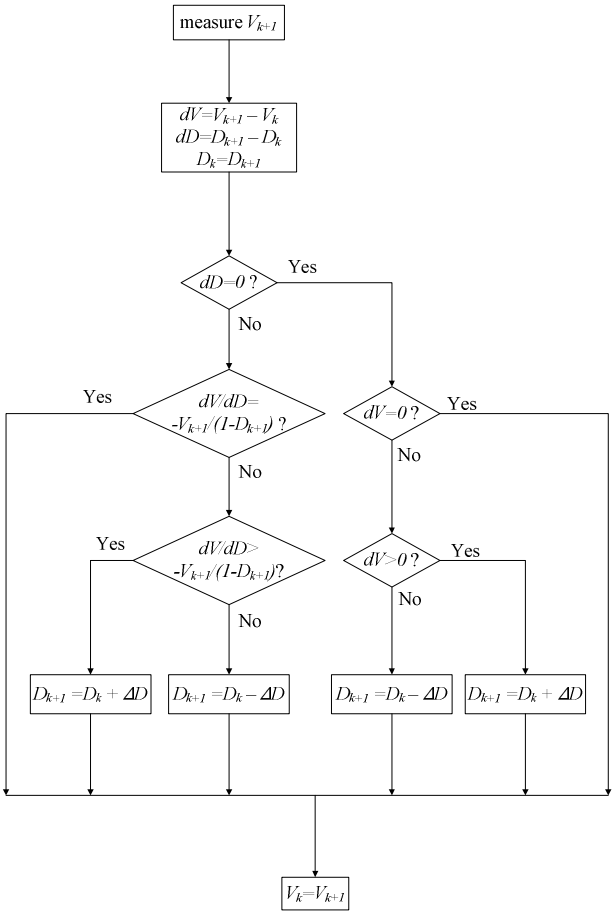

Fig. 1. ViSD algorithm control flow chart algorithm.

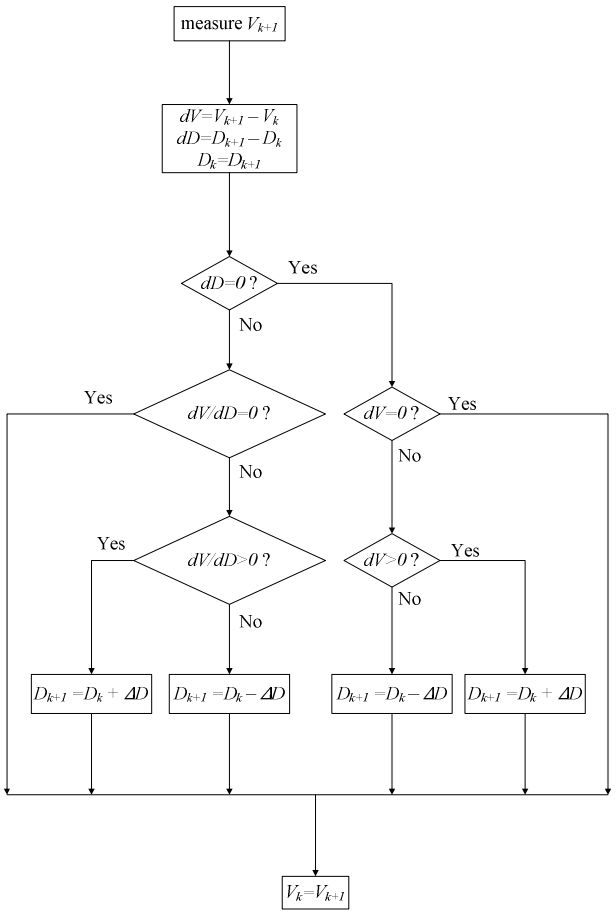

Fig. 2. VoSD algorithm control flow chart algorithm.

The control flow chart algorithms of the ViSD and VoSD techniques are similar to that of the INC method. However, the ViSD and VoSD techniques' flow chart algorithms sense only the solar panel voltage whereas the INC method control flow chart algorithm senses both the panel voltage and current.

III. IMPLEMENTATION

Fig. 3 and 4 show the Simulink circuits that were used in simulating the ViSD and VoSD algorithms respectively.

The Simulink implementation of the ViSD MPPT subsystem in Fig. 3, is shown in Fig. 5, and the Simulink implementation of the VoSD MPPT subsystem in Fig. 4, is shown in Fig. 6. The ViSD and VoSD Simulink implementations in Fig. 5 and 6 were derived from the control flow chart algorithms in Fig. 1 and 2 respectively.

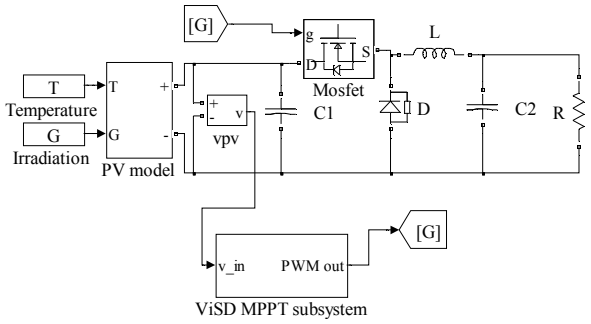

Fig. 3. Simulink circuit for simulating the ViSD technique.

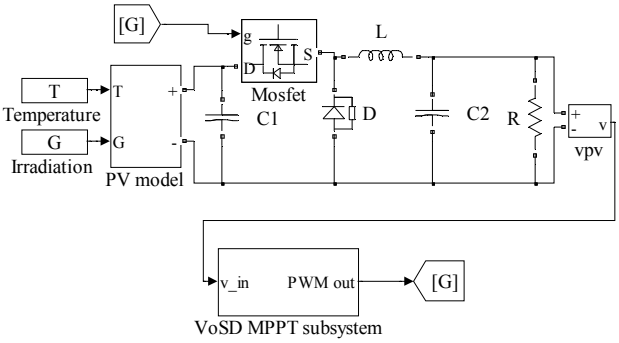

Fig. 4. Simulink circuit for simulating the VoSD technique.

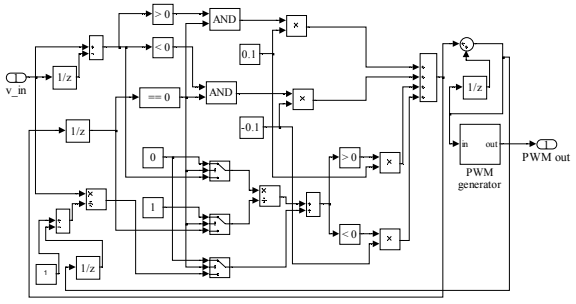

Fig. 5. ViSD algorithm Simulink implementation.

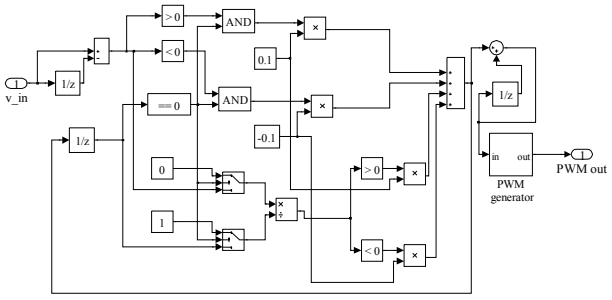

Fig. 6. VoSD algorithm Simulink implementation.

After simulations, experiments were carried out to validate the proposed techniques. An ASE-100-GT-FT multi-crystalline Scott solar panel was used for the experiments. The characteristics of the solar panel are below:

Power	100 Wp
V_{oc}	42.5 V
I_{sc}	3.2 A
V_{mpp}	34.5 V
I_{mpp}	2.9 A

Eight 500 W tungsten halogen lamps were used to provide constant insolation to the solar panel. The ViSD and VoSD algorithms' control systems were implemented using Texas Instruments TMS320F2812 DSP system. Fig. 7 and 8 show the ViSD and VoSD experimental circuits respectively.

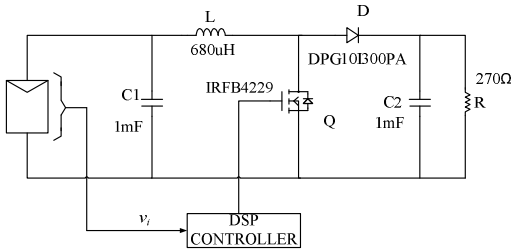

Fig. 7. ViSD algorithm experimental circuit.

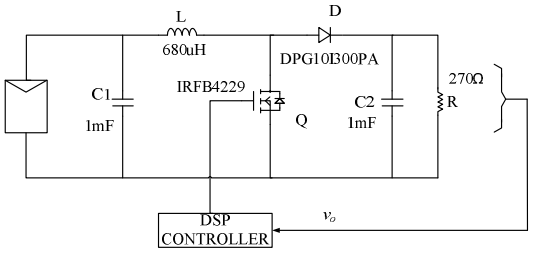

Fig. 8. VoSD algorithm experimental circuit.

The boost converters in Fig. 7 and 8 were first operated in the *I-V* curve-tracer mode so as determine the maximum power point of the solar panel. Thereafter, the ViSD and VoSD techniques were implemented so as to validate their effectiveness in tracking the MPP. The same experimental setup was used to implement the incremental conductance algorithm (INC) so as to compare the performance of the INC algorithm against the ViSD and VoSD algorithms.

IV. FINDINGS

A. Simulation results

To validate the ViSD and VoSD techniques in Simulink, the boost converter in Fig. 3 was first operated in *I-V* curve-tracer mode so as to obtain the *P-V* characteristic of the Simulink PV model. Fig. 9 shows the *P-V* characteristic; p_{pv} is the PV model output power and v_{pv} is the model output voltage. From Fig. 9, the PV model maximum power point power is 200 W.

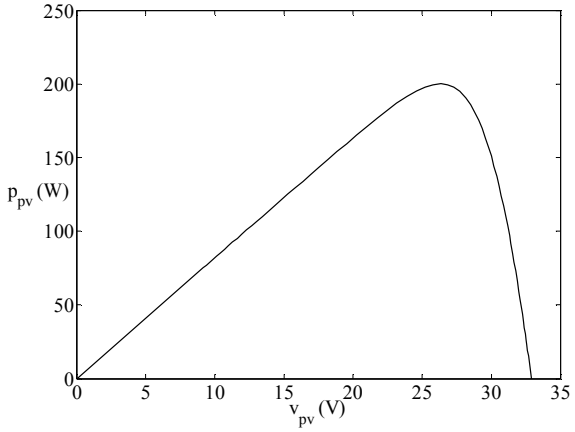

Fig. 9. *P-V* characteristic of the Simulink PV model.

Thereafter, the Simulink ViSD and VoSD techniques in Fig. 3 and 4 were simulated so as to track this maximum power point. Results of the maximum power point tracking are shown in Fig. 10 and 11.

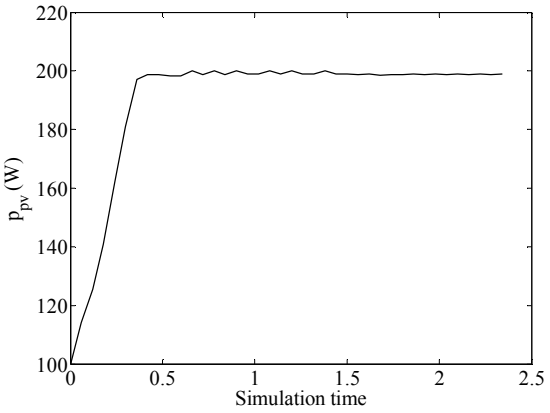

Fig. 10. ViSD algorithm tracking of the Simulink PV model MPP.

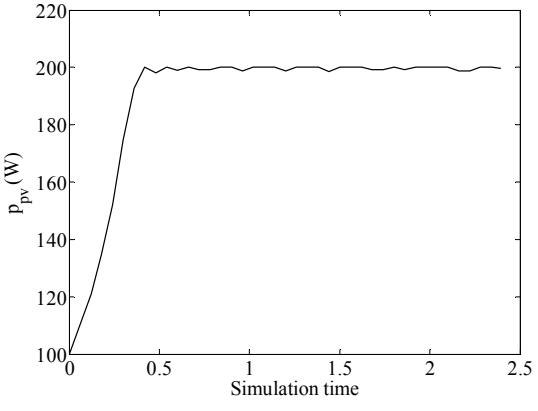

Fig. 11. VoSD algorithm tracking of the Simulink PV model MPP.

Fig. 10 and 11 show that the Simulink simulations of the ViSD and VoSD algorithms track the Simulink PV model maximum power point.

B. Eperimental results

1) ViSD algorithm

The ASE-100-GT-FT solar panel maximum power point — under illumination from eight 500 W tungsten halogen lamps — was first determined as 14.9 W, by operating the Fig. 7 boost converter in *I-V* curve-tracer mode.

Results of the maximum power point tracking by the ViSD algorithm are shown in Fig. 12; p_{pv} is the PV module output power. During the experiment, changes in irradiance were emulated by switching off, half of the tungsten halogen lamps for a short while.

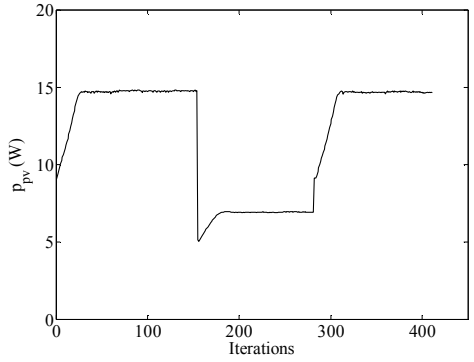

Fig. 12. ViSD algorithm tracking of solar panel MPP.

Fig. 12 shows that the ViSD algorithm tracks the ASE-100-GT-FT solar panel maximum power point.

Fig. 13 shows a comparison of the performances of the incremental conductance algorithm (INC — thin line) and the ViSD algorithm (ViSD — bold line) in tracking the ASE-100-GT-FT solar panel maximum power point. During the experiment, changes in irradiance were emulated by switching off, half of the tungsten halogen lamps for a short while.

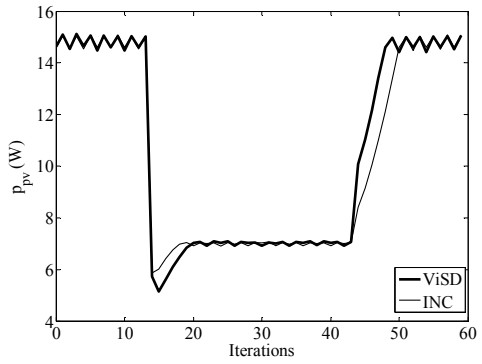

Fig. 13. INC and ViSD methods' MPPT performances.

Results of Fig. 13 show that the INC method and the ViSD algorithm deliver almost similar performances.

2) VoSD algorithm

By operating the Fig. 8 boost converter in *I-V* curve-tracer mode, the ASE-100-GT-FT solar panel maximum power point — under illumination from eight 500 W tungsten halogen lamps — was first determined as 15.5 W.

Results of the maximum power point tracking by the VoSD algorithm are shown in Fig. 14; p_{pv} is the PV module output power. During the experiment, changes in irradiance were emulated by switching off, half of the tungsten halogen lamps for a short while.

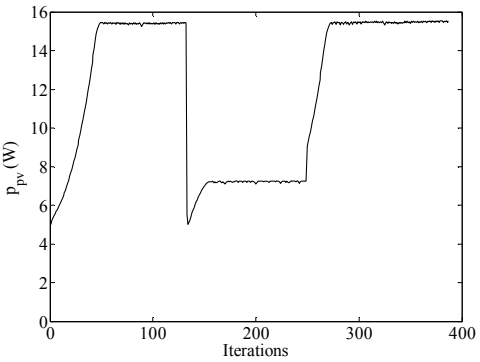

Fig. 14. VoSD algorithm tracking of solar panel MPP.

Fig. 14 shows that the VoSD algorithm tracks the ASE-100-GT-FT solar panel maximum power point.

Fig. 15 shows a comparison of the performances of the incremental conductance algorithm (INC — thin line) and the VoSD algorithm (VoSD — bold line) in tracking the ASE-100-GT-FT solar panel maximum power point. During the experiment, changes in irradiance were emulated by switching off, half of the tungsten halogen lamps for a short while.

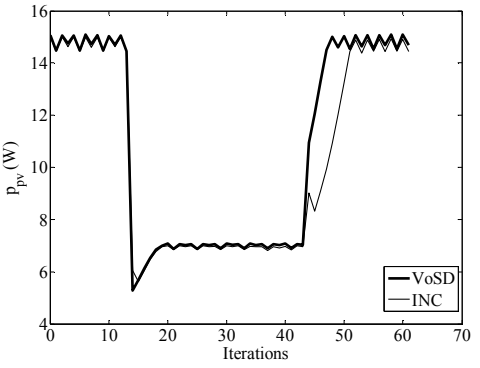

Fig. 15. INC and VoSD methods' MPPT performances.

Results of Fig. 15 show that the INC method and the VoSD algorithm deliver almost similar performances.

V. CONCLUSIONS

Two new maximum power point tracking algorithms — the ViSD and VoSD algorithms — whose operational characteristics and features are similar to those of the incremental conductance algorithm have been presented. Compared to the incremental conductance method, both the ViSD and VoSD algorithms eliminate the use of the more costly and complex current sensor, by using only the voltage sensor. This results in reduced costs and circuit complexity. Moreover, the VoSD technique is less complex; hence, it requires less computational processing.

ACKNOWLEDGMENT

The authors would like to thank the DHPA scheme for supporting this research work.

REFERENCES

[1] T. Esram and P.L. Chapman, "Comparison of Photovoltaic Array Maximum Power Point Tracking Techniques", *IEEE Transactions on Energy Conversion*, vol. 22, no. 2, pp. 439-449, June 2007.

[2] M. A. S. Masoum, H. Dehbonei, and E. F. Fuchs, "Theoretical and experimental analyses of photovoltaic systems with voltage and current-based maximum power-point tracking," *IEEE Trans. Energy Convers.*, vol. 17, no. 4, pp. 514–522, Dec. 2002.

[3] T. Noguchi, S. Togashi, and R. Nakamoto, "Short-current pulse based adaptive maximum-power-point tracking for photovoltaic power generation system," in *Proc. 2000 IEEE Int. Symp. Ind. Electron.*, 2000, pp. 157–162.

[4] E. Koutroulis, K. Kalaitzakis, and N. C. Voulgaris, "Development of a microcontroller-based, photovoltaic maximum power point tracking control system," *IEEE Trans. Power Electron.*, vol. 16, no. 21, pp. 46–54, Jan. 2001.

[5] M. A. Slonim and L. M. Rahovich, "Maximum power point regulator for 4 kWsolar cell array connected through invertor to the AC grid," in *Proc. 31st Intersociety Energy Conver. Eng. Conf.*, 1996, pp. 1669–1672.

[6] M.Veerachary, T. Senjyu, andK.Uezato, "Maximum power point tracking control of IDB converter supplied PV system," in *IEE Proc. Elect. Power Applicat.*, 2001, pp. 494–502.

[7] G. J. Yu, Y. S. Jung, J. Y. Choi, I. Choy, J. H. Song, and G. S. Kim, "A novel two-mode MPPT control algorithm based on comparative study of existing algorithms," in *Conf. Record Twenty-Ninth IEEE Photovoltaic Spec. Conf.*, 2002, pp. 1531–1534.

[8] K. Irisawa, T. Saito, I. Takano, and Y. Sawada, "Maximum power point tracking control of photovoltaic generation system under non-uniform insolation by means of monitoring cells," in *Conf. Record Twenty-Eighth IEEE Photovoltaic Spec. Conf.*, 2000, pp. 1707–1710.

[9] K.Kobayashi, I. Takano, andY. Sawada, "A study on a two stage maximum power point tracking control of a photovoltaic system under partially shaded insolation conditions," in *IEEE Power Eng. Soc. Gen.Meet.*, 2003, pp. 2612–2617.

[10] Y.-C. Kuo, T.-J. Liang, and J.-F. Chen, "Novel maximum-power-point tracking controller for photovoltaic energy conversion system," *IEEE Trans. Ind. Electron.*, vol. 48, no. 3, pp. 594–601, Jun. 2001.

[11] M. G. Simoes, N. N. Franceschetti, and M. Friedhofer, "A fuzzy logic based photovoltaic peak power tracking control," in *Proc. IEEE Int. Symp. Ind. Electron.*, 1998, pp. 300–305.

[12] T. Hiyama, S. Kouzuma, and T. Imakubo, "Identification of optimal operating point of PV modules using neural network for real time maximum power tracking control," *IEEE Trans. Energy Convers.*, vol. 10, no. 2, pp. 360–367, Jun. 1995.

[13] N. Mohan et al., *Power Electronics-Converters, Applications and Design*, Wiley, New York, 2003.

[14] A. Emadi et al., *Integrated Power Electronic Converters and Digital Control*, CRC Press, Boca Raton, 2009.